ARMA 17-009

Improving Hard Rock Pillar Design by Including Rock Mass Classification and Failure Mechanisms

Oke, Jeffrey
MDEng Inc., Kingston, Ontario, Canada
Esterhuizen, Gabriel S.
NIOSH-Pittsburgh Research Laboratory, Pittsburgh, Pennsylvania, USA

This paper was prepared for presentation at the 51st US Rock Mechanics / Geomechanics Symposium held in San Francisco, California, USA, 25-28 June 2017. This paper was selected for presentation at the symposium by an ARMA Technical Program Committee based on a technical and critical review of the paper by a minimum of two technical reviewers. The material, as presented, does not necessarily reflect any position of ARMA, its officers, or members. Electronic reproduction, distribution, or storage of any part of this paper for commercial purposes without the written consent of ARMA is prohibited. Permission to reproduce in print is restricted to an abstract of not more than 200 words; illustrations may not be copied. The abstract must contain conspicuous acknowledgement of where and by whom the paper was presented.

ABSTRACT: The limitations of the current pillar strength formulas, empirical design charts, and continuum numerical modelling is that these methods do not consider discontinuity driven failure mechanisms (i.e. jointing at critical angles). However, strength formulas have been very effective within the coal industry because they have a better representation of the rock mass strength (sample sizes > standard sizes) and large databases of case histories providing sufficient statistical representation of both stable and failed cases. Additionally, coal pillars generally have larger width to height ratio (>1) which decreases the influence of through going structure. This is opposite for hard rock mine where the width to height ratio is generally <2 and as small as 0.3, were structure can have a major influence on the stability. Additionally, the small size of hard rock unconfined compressive strength samples does not represent the strength of the rock mass, without additional considerations. Therefore, an improved strength formula is proposed that includes the influences of rock mass strength and discontinuities. This proposed strength formula, and its associated factors (length effect, and discontinuity dip and properties) can be used to create site specific empirical design charts.

1. INTRODUCTION

Following the Coalbrook Colliery pillar collapse disaster in 1960, there has been an increased need to improve pillar design. Since the disaster, many authors have contributed to developing/improving strength formulas (Eq. 1) and empirical design charts. Martin and Maybee (2000) and Oke and Kalenchuk (2017) provide an excellent summary of these empirical strength formulas and design charts. Martin and Maybee (2000) also provide some insight on pillar strength through their result of continuum numerical modelling However, these methods, and others do not consider specific failure mechanisms (i.e. structural vs stress) or do not have the same failure definition (i.e. functional/serviceability vs collapse). The need to consider structural failure mechanisms was addressed in a strength formula for limestone pillars (Esterhuizen et. al 2008a), but the empirically based procedure is applicable to limestone mines in the United States only (based on the dataset). Continuum numerical modelling does not capture structural failure mechanisms, unless the individual governing structure (e.g. a joint) is explicitly simulated, but can provide insight into the amount of expected yield. Depending on the amount (depth) of yield the pillar will be expected to collapse or meet serviceability thresholds. Even though an empirical technique will work for the given case study and very similar situations (Oke and Kalenchuk (2017), and Malan and Napier (2011)) conclude that neither empirical techniques nor numerical modelling can be used solely to provide a solid basis to predict pillar strength, σ_p. The authors of this paper, hypothesize that simple continuum numerical and current empirical equations can provide inaccurate results primarily due to the following two conditions: the dominant influence of critically oriented discontinuities at low width-to-height ratios and serviceability limits at larger width-to-height ratios, as shown in the hatched regions in Figure 1.

$$\sigma_p = K \cdot \frac{W^b}{H^a} \quad (1)$$

where:
K is the strength of a unit cube
W is the width of the pillar
H is the height of the pillar
a and b are curve fitting parameters (i.e. 0.75 and 0.5 respectively for hard rocks, Hedley and Grant, 1972)

Figure 1 illustrates the hypothesis that at low width to height ratios continuum numerical modelling will not satisfy equivalent continuum requirements (failure mechanisms can be discontinuity driven) therefore the

strength will be greater than observed (i.e. empirical) predictions. However, the design will be too conservative if each pillar is designed to an observed pillar with a through-going discontinuity that is uncharacteristic of the remainder of the mine. On the other end, when the width to height ratio is large, the results from numerical models can predict a stable pillar, while observed predictions will indicate an unstable pillar. There will be observed instability of pillars because stresses along the pillar walls will be too large, resulting in localized failure (i.e. squeezing, strain bursting, stress-induced damage). If these larger pillars are required to provide a safe travel way, they could be assessed as being too unstable and unsafe to operate beside, thus meeting its serviceability limit. When these pillars are vertical (major principal stress acting in the vertical direction), these pillars may be stabilized by the loose failed material around the pillar, providing a small amount of confinement. However, if the pillars are horizontal, the localized failure is able to fall away on the one side of the pillar, removing the small, but critical, amount of confinement that provided stability for the vertical pillar. The loss of confinement can ultimately lead to the failure of these horizontal pillars. Additionally, to mitigate this type of serviceability issues, support can be installed based on an analysis of the excavation, not of the pillar.

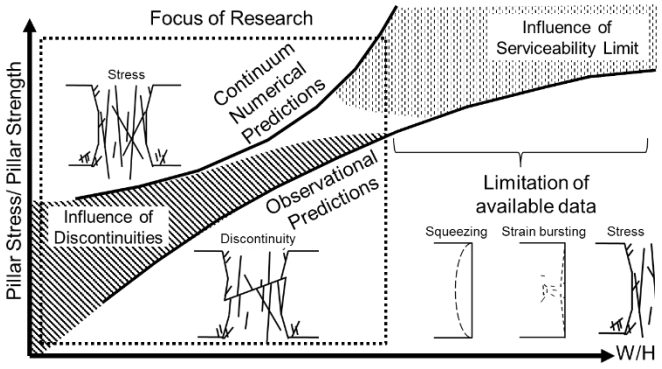

Fig. 1. Illustration of the discrepancy between continuum numerical predictions and observational (empirical) predictions. Where: W = pillar width, and H = pillar height

Examples of the serviceability limit as well as the difference between continuum numerical modelling and empirical equation are illustrated in Figure 2. The numerical model results come from the simulated brittle hard rock, two-dimensional (2D) analysis of Martin and Maybee (2000), which agrees well with other empirical work (involving sub vertical pillars) from hard rock mining (i.e. Hedley and Grant 1972) when the width to height ratio is below 1.5 (Martin and Maybee 2000). However, the numerical results diverge from the empirical strength formula solution of Hedley and Grant (1972) when the ratio increases past 1.5 as shown in Figure 2. These solutions have been normalized to the rock mass strength (σ_{cm}) to allow for a more accurate comparison, as further discussed in section 2.1.

The parameters used for the Hedley and Grant (1972) empirical solution, within Figure 2, were modified to a single case study presented by Labrie et al. (2007) where a 9m wide horizontal sill pillar violently collapsed . The authors assume that the gravity removed the small confinement on the underside of the pillar of the failed rock material around the pillar, resulting in the effective width diminishing and stress conditions increasing to the pillar's ultimate capacity. If this pillar was vertical, as were the ones used to calibrate the empirical solution, it is possible that the small amount of confinement, provided by the failed material that would have sloughed off would have kept it stable; however, there is limited data on pillar instability from this range of pillar width to height ratios (where the serviceability limit is reached), so it will no longer be discussed here. The focus of this paper will be testing the authors' hypothesis on the lower pillar width to height ratio (<2.0) where discontinuities can have a governing design factor as illustrated in Figure 1.

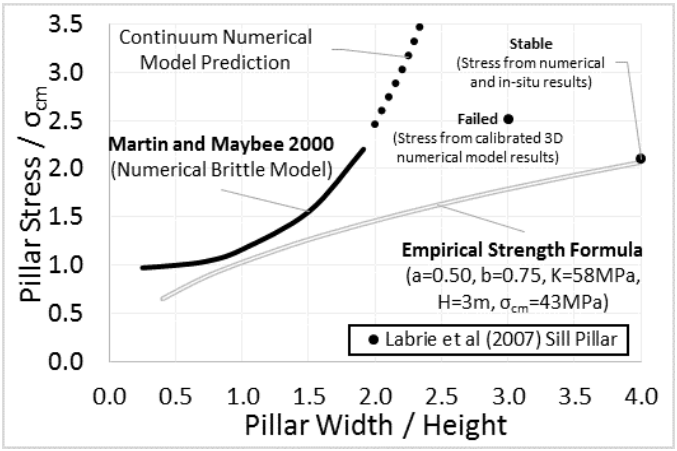

Fig. 2. The continuum 2D numerical (brittle parameters) model results of Martin and Maybee (2000) compared to empirical results of Hedley and Grant (1972) with the assumption of K=UCS/3 (Jager and Ryder, 1999). All results are normalized to the rock mass strength for the referenced material.

The aim of this paper is to improve hard rock pillar strength formula at low pillar width to height ratios through the inclusion of rock mass classification, consideration of post-peak behaviour, length of the pillar, critical joint dip and persistence. A proof of concept of the improved pillar strength formula will be compared to the stable and failed cases in the NIOSH limestone pillar database, (NIOSH, 2017). This paper will conclude with a pillar strength chart verified against the limestone database. This type of pillar strength chart could be created for any mine site as early as the feasibility stage, and further refined throughout operations.

2. IMPROVING PILLAR STRENGTH FORMULA

An improved pillar strength formula is proposed by the authors of this paper through the inclusion of rock mass

classification, length of the pillar, consideration of post-peak behaviour, critical joint dip and persistence. The improved pillar formula is shown in Eq. 2 and will be further explained in subsequent sections.

$$\sigma_p = DFM\ \sigma_{cm} \left(1 - \frac{H^{(b-a)}}{2^b} + \frac{W^b}{H^a}\right) \quad (2)$$

where:
DFM = Discontinuity factor multiplier
σ_{cm} = Rock mass strength
σ_p = Pillar Strength
a and *b* are curve fitting parameters to numerical analysis results

2.1. *Rock Mass Classification*

The aim of rock mass classification is to process information on rock material properties, discontinuity characteristics and excavation geometry to obtain representative values (rock mass strength, σ_{cm}) that provide a rational basis for rock engineering decisions (Priest, 2012). Hoek (2007) states that it is more useful in regard to pillar strength to have an estimate of the rock mass strength of the pillar rather than a detailed knowledge of the extent of fracture propagation in the pillar. Based on the previous references from literature and the success of large sample sizes (ft^3 to m^3) for the coal empirical strength formula and in-situ back-analysis, the strength of the pillar should be a function of the rock mass strength. The rock mass strength is a representative strength of the rock mass when the width to height ratio is ~0.5 (equivalent to a UCS width to height ratio, i.e. without confinement). Therefore the strength formula had to be modified (with inclusion of $1\text{-}H^{(b-a)}/2^b$) so that at a width to height ratio of 0.5, the pillar strength will be equal to the rock mass strength

2.2. *Influence of Length*

Many authors have attempted to validate the influence of length with respect to the strength of the pillar, as shown in Figure 3. Malan and Napier (2011) state that there is no good experimental evidence available regarding the effect of pillar shape on strength for hard rock pillars. Ryder and Ozbay's (1990) guidelines indicate that there is an insignificant increase of strength when the length of the pillar is greater than four times the width of the pillar. Esterhuizen et al. (2008a) found (through numerical simulations) that for pillars in hard brittle rock when the W/H≤0.5 there is no additional influence of the length on the strength. Additionally, Esterhuizen et al. (2008a) noted that when the width to height ratio is greater than 1.4 the hydraulic radius can be used to find an equivalent width (W_e, Eq. 3) of the pillar, as proposed by Wagner (1974). Esterhuizen et al. (2008a) provide a table for the transitions of the width to height ratio from 0.5 to 1.4. The solution of Esterhuizen et al. (2008a) was plotted within Figure 3 with a constant width to height ratio of 0.8. The authors of this paper have simplified the Esterhuizen et al. (2008a) length influence table to be expressed as a single equation (Eq. 4). Proper calibration of the influence of the length can be conducted through a series of three and two- dimensional numerical analyses while respecting the applicable design range for a given site. However, for feasibility studies any of the listed methods within Figure 3, can be used, provided that the rationale for the selection is included.

$$W_e = LBR \left(\frac{4A}{C} - W\right) + W \quad (3)$$

$$LBR = \frac{1}{1 + 5e5^{(0.8 - W/H)}} \quad (4)$$

Where:
A = Cross section area of the pillar
C = Perimeter of the cross section of the pillar

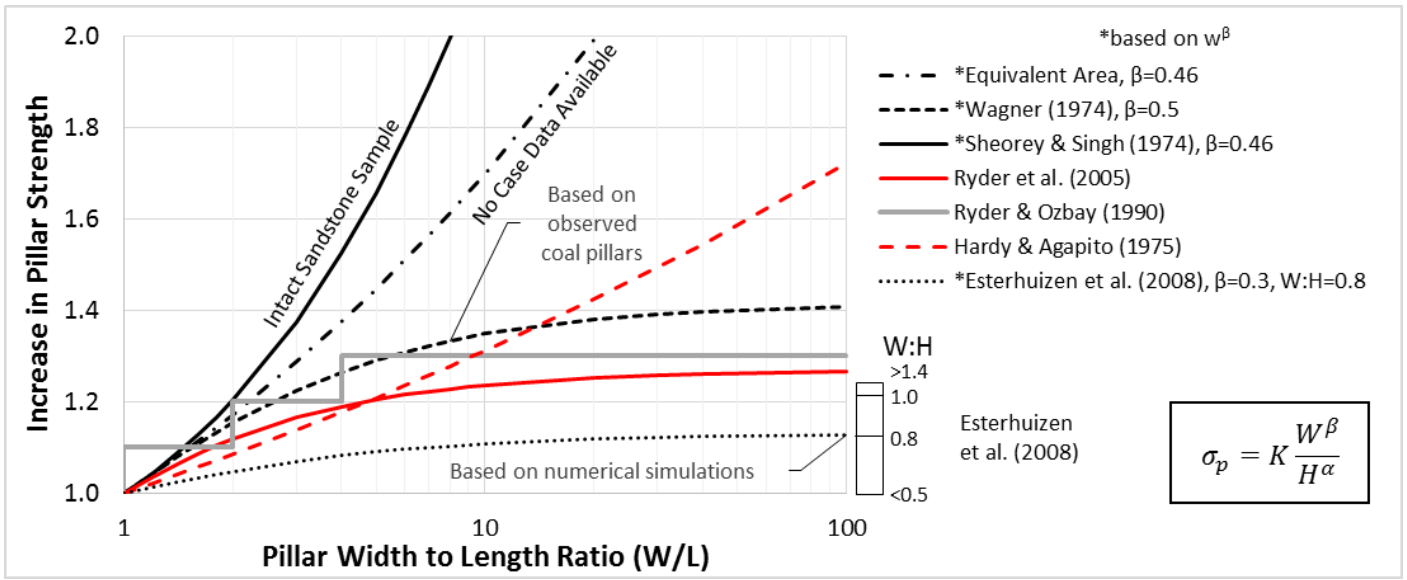

Fig. 3. Influence of length of the strength of the pillar. Lines in red denote reference from secondary source, please use only after review of original source.

2.3. *Inclusion of brittle/ductile rock mass and post-peak behaviour*

The inclusion of post-peak behaviour of the rock mass should be included in assessing the pillar behaviour. Hard rock masses of very good quality will have a brittle behaviour at low confinement, but should have strain hardening behaviour at higher confinement. However, very poor quality soft rock masses may display perfectly plastic behaviour. Rock mass classification can provide an estimate of material properties used for advanced numerical models. Advanced numerical models (i.e. three-dimensional, 3D, and/or discontinuum numerical modelling) can be used to validate the a and b parameters for Eq. 2. Simple 2D continuum numerical analysis, which assumes infinite long pillars, can approximate these parameters through inclusion of a length factor, as explained in the previous section. The authors found that 2D numerical brittle / strain hardening results of Martin and Maybee (2000), as shown in Figure 2, have *a* and *b* parameters of 5 and 3.5 respectively. These parameters were found after assuming no further increase of stress with length if the pillar is four times the width (Ryder and Ozbay, 1990) and by using Eq. 4. Additionally, the height of the pillar was assumed to be 10m.

2.4. *Adjustment for Discontinuities*

As illustrated in Figure 1, the influence of discontinuities can be the governing factor for the design of pillars. To incorporate the influence of discontinuities, the authors of this paper propose the inclusion of the analytical solution of Jaeger and Cook (1969) for discontinuities, Eq. 5. Theoretically, pillars should fail at the strength of the discontinuity, as defined by Eq. 5 and shown in Figure 4, when the discontinuities are through going (i.e. the discontinuity daylight on all sides of the pillar), and when $\sigma_d < \sigma_{cm}$.

$$\sigma_d = \frac{2C_d + 2\sigma_3 \tan\phi_d}{(1 - \cot\beta \tan\phi_d)\sin 2\beta} \qquad (5)$$

where:

C_d= Cohesion of the discontinuity

ϕ_d= Friction angle of discontinuity

β = Dip angle of discontinuity (0° = perpendicular to σ_1, 90° parallel to σ_1)

The limitation of this analytical solution, is that the weakening effect cannot be taken account for when the dip of the discontinuity, β is less than the friction angle of the discontinuity, ϕ_d. Numerical simulation conducted by Zhang et al. (2015), Esterhuizen (2014), and Iannacchione (1999) indicates that the pillar strength can be reduced up to 25% with a discontinuities dip of <30° or >80°. An analysis by Zhang et al. (2015) captured the influence of persistence of the critical joint (of a 3 joint set system) on the strength of the pillar, as shown in Figure 5. The results of Zhang et al. (2015) indicate two different conclusions. First, when the joint persistence is not large enough to be through going, the reduction of the strength due to the discontinuity is a fraction. Second, when the joint persistence << Pillar width the discontinuity has less of an influence on the ultimate strength, as the pillar will fail as a rock mass (i.e. stress induced failure of Figure 1).

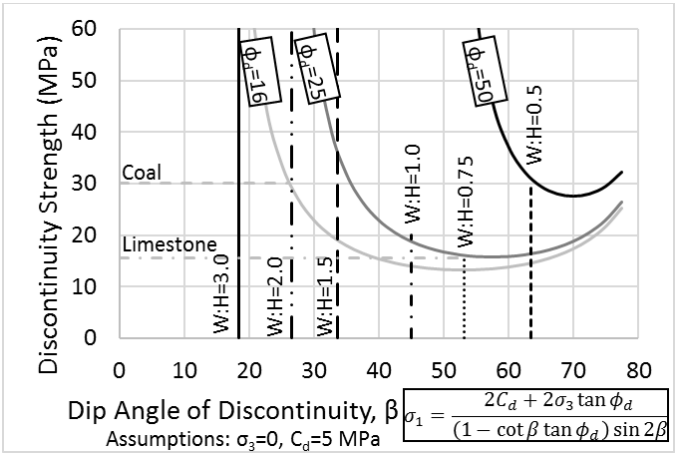

Fig. 4. Analytical solution of Jaeger and Cook (1969) for through-going discontinuities. The width to height ratio (W:H) line denote that maximum W:H ratio for the discontinuity to be through-going.

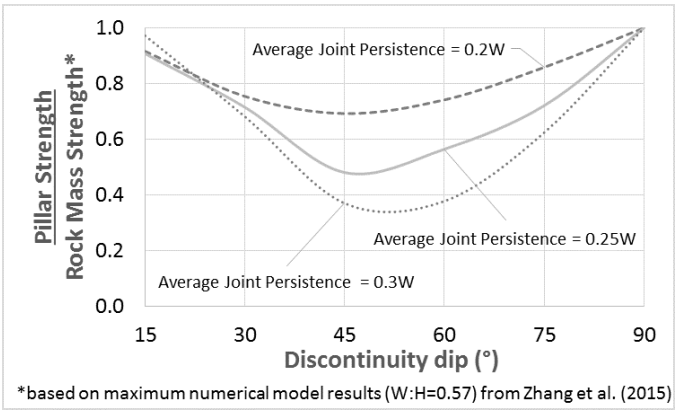

Fig. 5. Influence of discontinuity persistence on pillar strength. Modified after Zhang et al. (2015)

The authors' propose for discontinuity driven failures that the strength of the pillar will be that of the analytical solution when the width to height ratio is low enough for it to be through going, denoted as d_{min}. Discontinuity driven failure will no longer govern, once the width to height of the pillar reaches a certain width to height, denoted as d_{max}. This can be explained by the increase of confinement as the pillar width to height ratio increases (σ_3), which increases σ_d , which ultimately causes $\sigma_d > \sigma_{cm}$. Empirically and numerically, d_{max} has been inferred for the following scenarios as shown in Table 1. The d_{max} can be conservatively approximated by finding the width the height ratio where $\sigma_d = \sigma_{cm}$ for the critical discontinuity, then multiplying by a factor denoted M_d (example: M_d=2, Coal from Figure 4, assuming ϕ_d=16, σ_{cm}=30MPa). The d_{max} can be aggressively approximated by finding the width to height ratio of β_{crit} (β_{crit} = 45+ϕ_d/2) then multiplying by M_d (example. M_d=2, Limestone from

Figure 4, assuming ϕ_d=25°). The former, conservative approximation is not straightforward as there are two possible solutions. The authors have provided example design charts (Figure 6) in order to streamline the calculation (when it is possible to assume that there is zero confining stress (Figure 6A) or zero cohesion of the discontinuity (Figure 6B). Figure 6C provides an approximation of confining stress, based on the embedded empirical equation proposed by Lunder and Palkanis (1997). The Lunder and Palkanis (1997) solution is compared to the numerical work of Martin and Maybe (2000) for different lateral earth pressure coefficients, k. Martin and Maybe (2000) proposed that there is no increase of confinement when the width to height ratio is below 1. Similarly, Esterhuizen et al. (2008b) states that based on numerical modelling of brittle rock response there is evidence that pillars do not have any confinement below a width to height ratio of 0.8, as shown in the grey zone of Figure 6C. It is important to note that these design charts (Figure 6) do not find d_{min}, however, they find the W:H ratio that needs to be multiplied by M_d to find d_{max}. Based on the Coal and the Limestone database M_d = 2, however, this value still needs to be verified.

Table 1. Empirical and numerical inferred predictions of d_{max}.

d_{max}	Scenarios	Reference
1.5	Empirical: Limestone	Esterhuizen (2008b)
1.8	Numerical: Ubiquitous joint model	Lorig and Cabrera (2013)
2.0	Numerical: Brittle-strain hardening model of Canadian hard rock mines	Martin and Maybee (2000)
2.5	Numerical: Ubiquitous joint model of schistose rocks	Lorig and Cabrera (2013)
4.0	Empirical: Coal	Mark (2006)

The transition between d_{min} and d_{max} has been deemed to follow a logistic function / sigmoid function (Eq. 6) based on the previous findings of Zhang et al. (2015), Esterhuizen (2014), and Iannacchione (1999). The curve fitting parameter, A, that defines the shape of the function for Eq. 6 has been found to range from about 50 to 150 for limestone (based on NIOSH database).

$$DF = \frac{1}{1 + A^{(d_{ave} - W/H)}} \quad (6)$$

$$DFM = \frac{(\sigma_d - (\sigma_d - \sigma_{cm})DF)}{\sigma_{cm}} \quad (7)$$

where:
A = curve fitting parameter
$d_{ave} = (d_{min}+d_{max})/2$

There is substantial uncertainty with this curve fitting parameter, because the results are data limited for pillar width to height ratios of 1.0 to 1.5. For illustrative purposes, the A parameter will be assumed to be 100. This

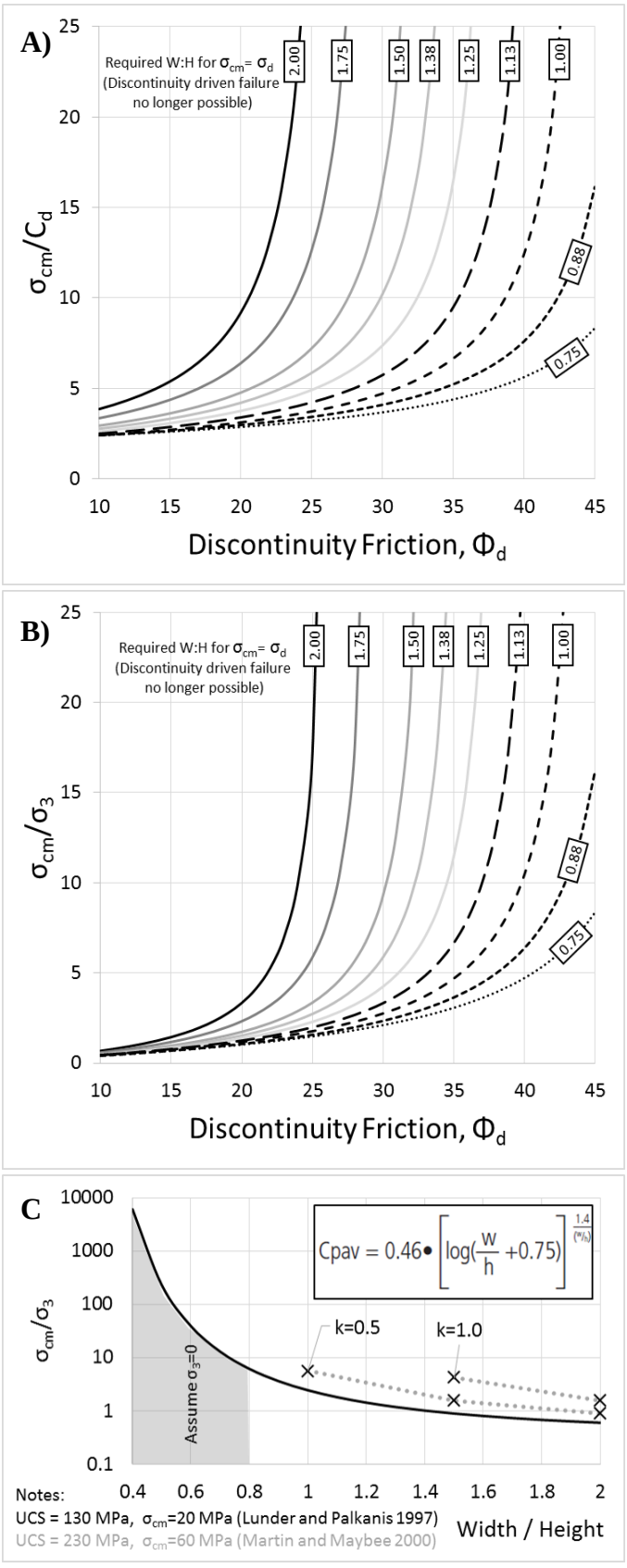

Fig. 6. Design charts for determining d_{max}. A) Assuming zero confinement. B) Assuming zero cohesion of discontinuity, and C) approximating confining stress based on width to height ratio. The x denotes the numerical results of Martin and Maybee (2000)

value still needs to be quantified for other rock mass types and conditions. Eq. 7, is the discontinuity factor multiplier for Eq. 2 so that the logistic function of Eq. 6 assigns the pillar strength of the discontinuity (σ_d) at d_{min}. At d_{max}, Eq. 7 approaches 1, so that the pillar strength would be defined by the stress strength line.

3. PILLAR STRENGTH CHART VERIFIED AGAINST LIMESTONE CASE HISTORIES

To illustrate each of the factors used within the improved empirical pillar strength formula, the solution will be verified against the limestone data base (Table 2) presented as a simplified design chart to mimic typical empirical pillar design charts for hard rock mines (Figure 7). Table 2 presents the failed limestone pillars in the NIOSH database, which includes minor modifications (as discussed below) as well as an approximated rock mass strength (σ_{cm}) based on the Hoek-Brown failure criterion (Hoek, 2007). In the NIOSH database "failed" pillars were defined as pillars that did not satisfy the requirement of providing safe access to the working area (Esterhuizen et al. 2008a). Of the failed pillars listed in Table 2, only one (case number 11) had collapsed, and the other pillars were all in various stages of deterioration requiring mining to be halted or extraordinary stabilization to be conducted because of unsafe conditions. These failed pillars were divided up into stress and discontinuity driven failures, with or without weak bedding, as shown in Figure 7. Stable (no signs of any damage) cases from the S-Pillar software program (NIOSH, 2017) were also plotted within Figure 7. These stable cases had their rock mass classification (GSI) reduced by 10, in order to justify the change that was applied for the weak-bedding, failed pillars, as discussed in the following sections. Table 3 presents the applicable ranges for NIOSH's stable and failed pillars database.

3.1. Database pillar strength adjustment

The following adjustments were made to the limestone database to obtain a better approximation of the rock mass strength of the individual failed pillars, as it was not always possible for NIOSH to conduct rock mass classification of the exact failed pillar because of the inherently hazardous conditions. The authors of this paper acknowledge that these adjustments factors have not been quantified, but represent a plausible minimum estimate, used to illustrate the importance of getting an accurate rock mass strength estimation.

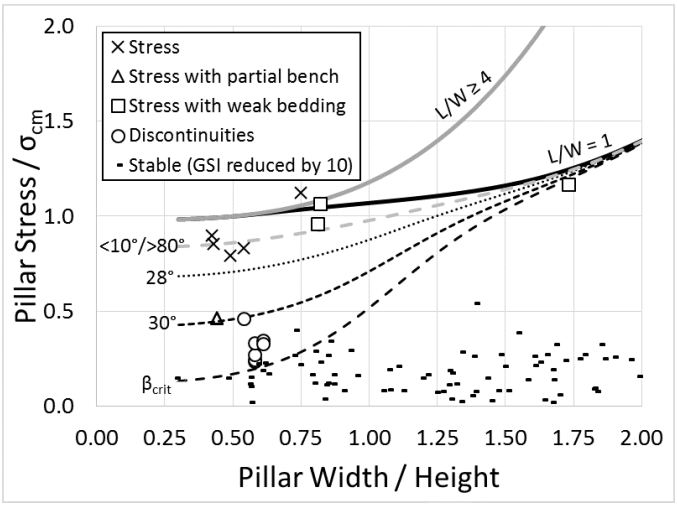

Fig. 7. Example pillar strength chart verified against limestone case histories with assumed GSI adjustments for failed pillars

Table 2. NIOSH modified failed pillar data base (NIOSH, 2017)

Case #	W (m)	H (m)	Stress (MPa)	GSI	Dip (°)	*UCS (MPa)	σ_{cm} (MPa)	Failure Type
1	10.7	18.3	9.0	69	55	214.9	38	Discontinuities
2	10.7	18.3	9.4	69	55	214.9	38	Discontinuities
3	10.7	18.3	10.3	69	55	214.9	38	Discontinuities
4	**11.6**	27.4	**18.4**	64	-	153.0	21	Stress
5	10.7	18.3	12.8	69	55	214.9	38	Discontinuities
6	12.2	27.4	17.2	75	-	150.0	37	Stress with partial bench
7	8.5	15.8	17.2	75	75	150.0	37	Discontinuities
8	12.2	27.4	17.3	75	-	150.0	37	Stress with partial bench
9	7.9	9.8	19.0	*73	-	160.0	**20	Stress with weak bedding
10	12.8	7.3	17.4	*73	-	160.0	**15	Stress with weak bedding / Scaling
11	12.5	15.2	17.8	*73	-	160.0	**17	Stress with weak bedding / Moisture
12	6.1	12.2	19.0	66	-	160.0	24	Stress
13	6.7	12.2	20.0	66	-	160.0	24	Stress
14	3.7	8.5	24.1	'64	-	214.9	28	Stress
15	8.2	9.1	25.0	*73	-	160.0	**20	Stress with weak bedding
16	5.5	7.3	27.0	66	-	160.0	24	Stress
17	**9.7**	15.8	**10.8**	70	60	164.8	31	Discontinuities
18	**9.7**	15.8	**10.2**	70	60	164.8	31	Discontinuities

Notes: *Based on average value at the mine, 'lowest value at the mine, **(bold)** denotes recent update to NIOSH database (S-Pillar, 2017 v1.03), **based on adjusted GSI

containing weak beds and moisture. Solid lines denote stress driven failure. Dashed lines denote discontinuity driven failure.

Weak bedding

Marinos and Hoek (2001) found that when a thin interlayer of weak siltstone was within a strong sandstone, GSI had to be reduced by 10. The failed limestone pillars with weak bedding were originally assigned by NIOSH a rock mass classification by extrapolating pillar assessments from nearby pillars. They did not take into consideration the potential for localized weak bedding in individual pillars. To introduce an adjustment factor for the presence of weak beds between stronger beds, the rock mass classification was reassigned with the average value for the individual mine (based on available data) then reduced to account for the assumption that the weak beds were more prominent in the individual pillars that failed than elsewhere in the panel. The reduction was equivalent to reducing GSI by 10. This reduction factor was based on following the methodology for selecting a GSI for heterogeneous rock masses (Marinos and Hoek 2001).

Table 3. Design parameter range of the NIOSH database

Design parameters		All pillars	Failed pillars
Height, H	Min	4.8	7.3
	Max	38.0	27.4
Width, W	Min	4.6	3.7
	Max	21.5	15.2
W/H	Min	0.3	0.4
	Max	3.5	1.8
GSI	Min	58.0	58.0
	Max	84.0	75.0

Moisture

Upon reviewing the rock mass classification, it was found that dry conditions were assumed. However, one of the pillars that failed was given the description of "moist". Therefore, the rock mass classification for all the failed pillars associated with moisture was reduced to take into consideration the influence of moisture. The reduction was equivalent to reducing GSI by 5. This reduction is based on the GSI description that states that a shift to the right (of the design chart) may be made for wet conditions (Marinos and Hoek 2001).

3.2. Pillar strength curve

Figure 7 shows the stress strength line, when the pillar is expected to fail by stress not by discontinuities, for when the length to width ratio (L:W) is equal or greater than 4 was based on the numerical results of Martin and Maybee (2000). A back-calculation was conducted in order to obtain the strength line for a square pillar, using Eq. 3 and Eq. 4. The stress and stress with weak bedding induced failed pillars all plot near or above the low/steep dipping discontinuity line, which makes sense because the limestone had sub-horizontal bedding that would interact with the failure. The only outliers were cases 6 and 8 which were both stress induced failure of pillars that were partially benched.

Discontinuity strength lines were developed based on the analytical solution of Jaeger and Cook (1969), assuming ϕ_d=25°, C_d = 1MPa, and σ_3=0. Additional discontinuity strength lines were added to take into account through going low angle joints and persistent steep dipping discontinuities, as numerically captured in Esterhuizen (2014), and Iannacchione (1999). The discontinuities all plot below the 30° dip and above β_{crit},≈57.5° which generally agrees with the measured discontinuities dips.

4. PROCEDURE OF IMPROVE HARD ROCK PILLAR DESIGN

The following section will describe the proposed procedure, of the authors of this paper, to improve the hard rock pillar design. Multiple options are provided with the most accurate option stated first, unless stated otherwise. However, it is important to keep in mind that the accuracy of the option used depends on the quality of the input parameters. The following is the step-by-step procedure to create a pillar design chart, based on Eq. 2.

- **(i)** A geotechnical investigation must be carried out to provide a rock mass classification and estimate the post-peak behaviour. This can be done through:
  - **(a)** Underground mapping
  - **(b)** Core logging
  - **(c)** Surface mapping
- **(ii)** Perform a numerical analysis of typical pillar sizes to calibrate *a* and *b* parameters to create the stress strength line (Eq. 2, *DFM* = 1). This can be done through:
  - **(a)** 3D analysis on square, and rectangular pillars
    - **(i)** If 3D analysis is conducted on square pillars, influence of length (see Section 2.2) can be used to estimate the effects of longer pillars
  - **(b)** 2D analysis (infinite length pillars)
    - **(i)** Influence of length (see Section 2.2) can be used to estimate the effects of square pillars
- **(iii)** Make an adjustment for critical discontinuity, discontinuity strength line (*DFN* = Eq. 7). Eq. 6 parameters can be found by:
  - **(a)** 3D numerical analysis with synthetic rock mass to establish *A*, d_{min} and d_{max}.
  - **(b)** 2D numerical analysis with synthetic rock mass to estimate *A*, d_{min} and d_{max}.
  - **(c)** The d_{min} can be estimated based on the width to height ratio so that a discontinuity dip at β_{crit} would no longer be through going.
  - **(d)** The d_{max} can be estimated (not is order of accuracy):
    - **(i)** Conservatively: Using the width to height ratio where σ_d=σ_{cm} for the critical discontinuity, then multiplying by a factor denoted M_d

(a) Use Eq. 5
(b) Use the design charts of Figure 6
(i) Assume zero confinement (Figure 6A)
(ii) Assume zero cohesion, then estimate σ_{cm}/σ_3 from Figure 6C, to use in Figure 6B

(ii) Aggressively: Based on d_{min} (from point c) multiplied by the factor M_d. It is important to note that $M_d = 2$ based on literature of Coal and the Limestone mines.

(e) Assume $A = 100$

(iv) Make adjustment for additional discontinuities
(a) Based on the other typical joint sets found at the mine from the geotechnical investigation.

(v) If required, a design chart can be made by assuming a typical height. Multiple design charts can be created for different potential multiple heights of pillars that may be encountered.

If numerical calibration is conducted for the given project, these parameters found from the calibration exercise could be used to supplement that geotechnical investigation. For example, if the persistence of a critical joint is significantly less than the width of the pillar, than an advanced numerical model could quantify the increase in the pillar strength of a critical discontinuity because failure would have to occur through intact rock (i.e. fracture propagation or bridging) as shown in Zhang et al. (2015).

5. CONCLUSIONS

The proposed improved pillar strength formula presented in this paper allows engineers to incorporate the failure mechanism into the design process. All the components required for the strength formula can be developed during feasibility study, and then modified and updated during operations to allow for further optimization of the strength equation. Furthermore, the improve strength equation can be expressed as a design chart, as shown in Figure 7, to allow for quick assessments of pillar stability when underground, if similar pillar heights are encountered. This paper will conclude with a description of the limitation of this method and the proposed future work, to ensure that readers/designers will understand them and be careful to use the proposed solution only within scope.

5.1. Limitations and Future Work

The following are limitations of the proposed improved strength formula and will be further researched in future work:

- The proposed method was developed for vertical square and rectangular pillars, which have four free faces. This method should not be used for stope pillars as they may have different design criteria (different failure modes)
- The proposed method does not consider the influence of roof or floor failure on the stability of the pillar.
- Stress induced failure design parameters (*a* and *b*) were derived from a generic numerical model results of Martin and Maybee (2000)
  - Design parameters can be found through two or three-dimensional numerical analysis as explained within this paper
- The limestone pillar strength chart was verified against the database of NIOSH, with the various ranges presented in Table 3.
- The proposed method does not consider the influence of persistence of the joints without the inclusion of advanced numerical models.

6. ACKNOWLEDGEMENT

The authors would like to acknowledge Ms. Palleske, Dr. Ghazvinian, and Mr. Lausch of MDEng for their contributions through discussions in the development of this paper.

7. DISCLAIMER

The findings and conclusions in this report are those of the authors and do not necessarily represent the views of the National Institute for Occupational Safety and Health. Mention of any company or product does not constitute endorsement by NIOSH.

8. REFERENCES

1. Esterhuizen G.S., D.R. Dolinar and J.L. Ellenberger 2008a. Pillar Strength and Design Methodology for Stone Mines. *Proc. 27th Int. Symposium on Ground Control in Mining*. Morgantown, WV: West Virginia University: 241-253.
2. Esterhuizen, G.S., D.R. Dolinar and J.L. Ellenberger. 2008b Assessment of stable and failed pillars in underground limestone mines. *Mining Engineering*, Nov; 60(11)
3. Esterhuizen, G. S. 2014. Extending empirical evidence through numerical modelling in rock engineering design. *Journal of the Southern African Institute of Mining and Metallurgy*, 114(10), 755-764.
4. Hedley, D.G.F. and F. Grant 1972 Stope-and-pillar design for Elliot Lake Uranium Mines. *Bulletin of the Canadian Institute of Mining and Metallurgy*, vol. 65, pp. 37–44.
5. Hoek, E 2007 *Practical rock engineering*. Rocscience Inc, North Vancouver
6. Iannacchione, A. T. 1999. Pillar design issues for underground stone mines. *In Proceedings of the 18th International Conference on Ground Control in Mining*, pp. 271-281.
7. Jaeger, J.C. and N.G.W. Cook 1969 *Fundamentals of Rock Mechanics*. London: Chapman and Hall.
8. Jager, A.J., and J.A. Ryder 1999 *A Handbook on Rock Engineering Practice for Tubular Hard Rock Mines*
9. Labrie, D., R. Boyle, T. Anderson, B. Conlon & K. Judge 2007 Monitoring the behavior of a sill pillar at

failure in a narrow-vein mine. Rock Mechanics: Meeting Society Challenges and Demands, 1385-1393.

10. Lorig, L.J., and A. Cabrera. 2013 Pillar strength estimates for foliated and inclined pillars in schistose material.
11. Lunder, P.J., and R. Pakalnis. 1997 Determination of the strength of hard rock mine pillars. *Bulletin of the Canadian Institute of Mining and Metallurgy*, vol. 68, pp. 55–67.
12. Malan D.F., J. A. L.Napier. 2011 The design of stable pillars in the bushveld complex mines: A problem solved?. *The Journal of the Southern African Institute of Mining and Metallurgy*, 111: 821–836.
13. Marinos P, and E. Hoek. 2001 Estimating the geotechnical properties of heterogeneous rock masses such as flysch. *Bull Eng Geol & the Environment* (IAEG), 60, 85-92
14. Mark, Christopher. 2006 The evolution of intelligent coal pillar design: 1981–2006. *In Proceedings of the 25th International conference on ground control in mining.* West Virginia University, Morgantown, pp. 325-334.
15. Martin, C.D. and W.G. Maybee, 2000 The strength of hard rock pillars, *International Journal of RockMechanics and Mining Sciences*, vol. 37, pp. 1239–1246.
16. NIOSH, S-Pillar 2017 http://www.cdc.gov/niosh/mining/works/coversheet1817.html v1.03
17. Oke, J. and K. Kalenchuk 2017 Selecting the Most Applicable Empirical Pillar Design. *ARMA* San Francisco, USA. (Paper Submitted)
18. Priest, S.D. 2012 *Discontinuity Analysis for Rock Engineering*. Springer Science & Business Media
19. Ryder, J.A. and M.U. Ozbay 1990 A methodology for designing pillar layouts for shallow mining. International Symposium on Static and Dynamic Considerations in Rock Engineering, Swaziland, ISRM.
20. Sheorey, P.R., B. Singh. 1974 Strength of Rectangular Pillars in Partial Extraction. *International Journal of Rock Mechanics and Mining Sciences*. 11:41-44.
21. Wagner, H. 1974 Determination of the complete load-deformation characteristics of coal pillars. 3rd ISRM Conference, vol. IIB, pp. 1076–1081.
22. Zhang, Y., D. Stead, D. Elmo. 2015 Characterization of strength and damage of hard rock pillars using a synthetic rock mass method. Computers and Geomechanics, 65: 56-73.